

# *Simulation Optimization and Finite Element Analysis of FSAE Racing Car Front Suspension*

Hongrui Kou<sup>a,\*</sup>, Bo Wu<sup>b</sup>, Jingkai Li<sup>c</sup>

*School of Mechanical & Power Engineering, Harbin University of Science and Technology,  
number 52 XueFu Drive, Harbin, China*

*a. khr1230@163.com, b. 869871621@qq.com, c. lijingkai2533@163.com*

*\*corresponding author*

**Keywords:** FSAE Racing, Front Suspension, Simulation Optimization, Finite Element Analysis

**Abstract:** The suspension is an important part of the FSAE racing car, and its rational design and optimization can significantly improve the smoothness and handling stability of the car. In this paper, the front suspension of the FSAE racing car is taken as the object of study, and its parameter design, simulation optimization, and structural analysis are carried out. Firstly, the front suspension of the FSAE racing car is selected according to the car layout and the requirements of the competition rules, the main parameters of the suspension are designed, and the suspension geometry is modeled by CATIA based on the design results. Secondly, a simulation model of the front suspension of the racing car was established by ADAMS/Car, and the parameters affecting the performance of the front suspension, such as front wheelbase, front beam angle, and front suspension camber coefficient, were simulated and analyzed. Then ADAMS/Insight is used to optimize the unreasonable parameters among them. Finally, this paper conducts a static study of the suspension and finite element analysis of the more complex column in the front suspension of the FSAE racing car through ANSYS. By analyzing the deformation and stress clouds of the left and right columns under braking and steering conditions respectively, it shows that the structure and materials of the left and right columns meet the design requirements.

## **1. Introduction**

Since its inception in 2010, the China Formula Student Car Competition has been increasingly sought after by domestic universities and students. The rules of the competition require teams to design and build a formula car with good handling, power, safety and reliability in accordance with the rules of the competition within a specified time. As an important part of a formula car, the suspension system is designed to absorb the impact loads of the car on uneven roads and attenuate vibrations. It transmits the forces and moments between the wheels and the frame to ensure the smoothness and handling stability of the vehicle. Therefore, simulation analysis and design optimization of the racing car suspension system is crucial. In this paper, we will establish a three-dimensional model of the front suspension of a formula car using CATIA, and use the Car module of ADAMS software for kinematic simulation analysis, then optimize the design of the front suspension system in ADAMS/insight module, and finally calibrate some components of the front suspension wheel side system through ANSYS

finite element analysis to make it more reasonable for the arrangement of the whole car. The design of the front suspension system is then optimized in ADAMS/insight module.

## 2. Design of FSAE Racing Front Suspension

### 2.1. The Basic Process of FSAE Racing Suspension Design

The design process for the front suspension of the race car in this paper is as follows:

- ① Selection of the structural form of the suspension, usually using unequal length double wishbone suspension, the difference being the choice of tie rod or push rod form;
- ② First select the basic parameters of the race car, including overall vehicle weight, overall vehicle size, front and rear axle load distribution;
- ③ Selection of the size of the offset frequency and four-wheel alignment parameters for the front and rear of the car;
- ④ Deriving the suspension stiffness and spring elasticity coefficients of the race car from the above parameters;
- ⑤ A calculation of the suspension stiffness to see if the car needs to be designed with anti-roll bars;
- ⑥ Calculation of lateral load transfer distribution for racing cars not designed with anti-sway bars;
- ⑦ Final determination of the damping rate of the shock absorber;
- ⑧ Simulation analysis of the positioning parameters of the racing car, the height of the center of lateral inclination, and optimization of the unqualified parameters;
- ⑨ Finite element analysis of the structure of each rod;
- ⑩ The result is a set of FSAE front suspensions that meet race standards.

### 2.2. Selection of Suspension Types for FSAE Racing

The double-wishbone independent suspension is characterized by the use of upper and lower wishbones of suitable size ratio, and the angle and wheelbase of the wishbone can not change much with the main pin during the upward and downward tire travel, so the double-wishbone independent suspension is usually used in racing cars. The double-wishbone suspension arms are connected to the column at one end and to the frame at the other end. By choosing the right size ratio of the upper and lower wishbones, and by carrying out a proper layout, the steering wheel alignment parameters and wheelbase can be ensured to stay within the proper range, and the race car can have good stability.

Based on the suspension requirements of the competition rules, and taking into account the difficulty of processing and debugging of the suspension, we finally used a tie rod unequal length double-wishbone independent suspension for the front suspension of our car.

### 2.3. Determining the Main Parameters of FASE Racing

The basic parameters related to the FSAE race cars studied in this paper are shown in the following table:

Table 1: Basic parameters of the whole car of FSAE racing car.

| Parameters                  | Numerical Value |
|-----------------------------|-----------------|
| Track width /mm             | 1620            |
| Wheelbase (front/rear) / mm | 1128            |
| Total length /mm            | 2950            |
| Total height /mm            | 1350            |
| Displacement /ml            | 620             |

|                                       |                        |
|---------------------------------------|------------------------|
| Overall vehicle mass /kg              | 310                    |
| Maximum speed / ( $km \cdot h^{-1}$ ) | 120                    |
| Minimum Ground Clearance /mm          | 30                     |
| Inhalation form                       | Naturally aspirated    |
| Fuel tank volume /L                   | 5.0                    |
| Total mass (kg)                       | 385                    |
| Differential form                     | DrexlerV3 differential |
| Front and rear axle load distribution | 45/55                  |

### 2.3.1. FSAE Racing Front Suspension Off Frequency

The suspension and the spring-loaded mass constitute the inherent frequency (also called the bias frequency) of the vibration system, which is one of the main parameters that have a significant impact on ride comfort. It is one of the main parameters that have a relatively large impact on the ride comfort and is also one of the basic parameters of suspension design. The front suspension bias frequency of a car can be expressed by the following formula:

$$n = \sqrt{k/m} / (2\pi) \quad (1)$$

Where:  $k$ —Stiffness of the front suspension( $N/cm$ ); $m$ —Spring Load Mass of Front Suspension ( $kg$ ).

The selection of bias frequency should follow the following principles: ① general car for the consideration of smoothness, by the front low and then high; ② different front and rear bias frequency can prevent resonance; ③ based on the handling stability of racing cars, usually the front high and then low.

Table 2: The range of bias frequency values for different types of cars.

| Car Type                   | Frequency bias (Hz) |
|----------------------------|---------------------|
| Ordinary car               | 0.5~1.5             |
| Moderate negative lift car | 1.5~2.0             |
| High lift car              | 3.0~5.0 above       |

The bias frequencies of cars with different uses are different, and the general distribution is shown in Table 2 above. Referring to the bias frequency of F1 car is usually chosen 5Hz, considering the ability of F1 driver, the bias frequency of FSAE car is generally taken lower but larger than that of ordinary car. Considering the comprehensive appeal factors, the front suspension bias frequency of this paper is initially set as:  $n=2.8Hz$ .

### 2.3.2. FSAE Racing Suspension Stiffness Calculation

① Total stiffness  $K$  (multiplied by the appropriate stiffness)

The total stiffness of a racing car is the vertical force on the wheel contact point with respect to the unit vertical displacement of the body or frame. The front suspension ride stiffness of the race car studied in this paper can be obtained from the following equation.

$$K = 4\pi^2 n^2 m_c / 2 = 4 \times 3.14^2 \times 2.8^2 \times 143.5 / 2 = 22184.9 \quad (2)$$

Where:  $n$ —the offset frequency of the front suspension of the race car;  $m_c$ —the spring-loaded mass of the front suspension of the race car.

## ② Suspension stiffness

Suspension stiffness is the vertical force applied to the center of the wheel in unit vertical displacement relative to the body or frame. The total stiffness was obtained after the tandem combination of tire and suspension, minus the stiffness of the tire to get the suspension stiffness. From the following equation:

$$\frac{1}{K} = \frac{1}{K_s} + \frac{1}{K_w} \Rightarrow K_s = \frac{K_w \cdot K}{K_w + K} \quad (3)$$

Where:  $K_s$  is the suspension stiffness,  $K_w$  is the tire radial stiffness.

The radial stiffness of the tire is known to be  $K_w = 370000 \text{ N/m}$ . The stiffness of the front suspension can be obtained from the calculation of (3) as follows:

$$K_s = 370000 \times 22184.9 / (350000 - 22184.9) = 25039.8 \text{ (N/m)} \quad (4)$$

### 2.3.3. Suspension Damping Calculation

The damper damping factor for the suspension section can be calculated by the following equation:

$$\zeta = 4\pi \cdot m_c \cdot n \cdot \varphi \quad (5)$$

Generally speaking, a larger relative damping coefficient is chosen for the shock absorber reset and a smaller relative damping coefficient  $\varphi_c$  for the compression. Choosing larger damping  $\varphi_b$  for the reset stroke can accelerate the damping of vibration while choosing smaller damping for the compression stroke can reduce the impact force on the car due to the uneven road surface. Therefore, we choose the relative damping coefficients of rebound and compression for the FSAE race car:  $\varphi_b = 0.5$ ,  $\varphi_c = 0.4$  respectively. Therefore, there are:

Front suspension compression damping coefficient:

$$\zeta = 4\pi m_c n \varphi_c = 2018.64 \text{ Ns/m} \quad (6)$$

Front suspension rebound damping coefficient:

$$\zeta = 4\pi m_c n \varphi_b = 2523.3 \text{ Ns/m} \quad (7)$$

## 3. FSAE Racing Car Front Suspension Simulation Analysis and Optimization

### 3.1. Modeling of The Front Suspension

During the driving process of FSAE racing car, the tires will be impacted by the uneven road surface, while the body will produce side or longitudinal tilt, all of which will make the wheels jump up and down. Therefore, the front suspension needs to be established in the Adams software for parallel wheel hop simulation analysis to be established for the component hard points as shown in Table 3.

The rear suspension model is built according to the above hard points and the suspension assembly of the front suspension is built, as shown in Figure 1:

Table 3: Coordinates of each hard point of the front suspension.

| Hardpoint Name | Coordinate values (X,Y,Z) | Properties   |
|----------------|---------------------------|--|
| Uca_front      | (- 766, - 200.05, 263.15) | The front connection point between the upper cross arm and frame |
| Uca_rear       | (- 258, - 200.05, 263.15) | The rear connection point between the upper cross arm and frame  |
| Uca_outer      | (- 512, - 614.1, 283)     | The connection point of the upper cross arm to the column        |
| Lca_front      | (- 766, - 219.1, 21.85)   | The front connection point of lower wish-bone to frame           |
| Lca_rear       | (- 258, - 219.1, 21.85)   | The rear connection point between lower cross arm and frame      |
| Lca_outer      | (- 512, - 716, 27.4)      | The connection point between lower cross arm and column          |
| Prod_out-board | (- 461.2, - 689, 2.8)     | The connection point between tie rod and upper cross arm         |
| Prod_inboard   | (- 435.8, - 254, 447.3)   | The connection point between tie rod and rocker arm              |
| Damper_outer   | (- 385, - 203, 472.2)     | The connection point between shock absorber and swingarm         |
| Damper_inner   | (- 131, - 203, 472.7)     | The connection point of shock absorber to frame                  |
| Wheel_center   | (- 512, - 700, 155.2)     | Center point of wheel  |
| Tierod_outer   | (- 415, - 650, 77.4)      | The connection point of steering crossbar and column             |
| Tierod_inner   | (- 415, - 304.8, 77.4)    | Disconnection point of steering cross-rod                        |

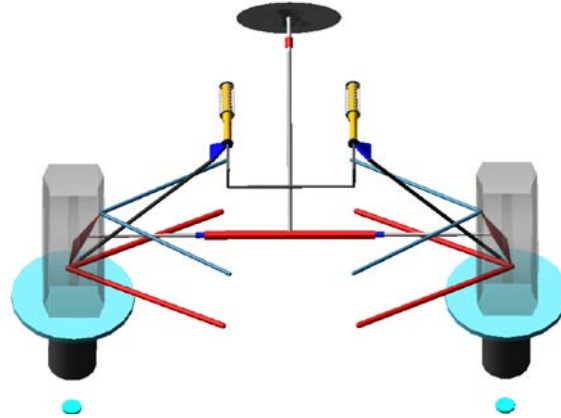


Figure 1: Total front suspension configuration.

### 3.2. Simulation Analysis of The Front Suspension

During the driving process of FSAE racing cars, the tires will be impacted by the uneven road surface, while the body will produce side or longitudinal tilt, which will make the wheels jump up and down. Therefore, the two-wheel bounce simulation produces changes in suspension parameters that can be

used as an important reference for analyzing the suspension performance. In this paper, through Adams/Car simulation, the up-and-down runout travel of the wheels is set to  $\pm 30\text{mm}$ , and the simulation curves of each parameter are obtained as follows:

### ● Front beam angle

The front beam angle decreases or increases when the wheel bounces up and down, both of which will be achieved in the understeer during the turn. However, the front beam angle changes too much during wheel hopping, which will cause sliding friction from tire side deflection, intensifying tire wear and poor straight-line driving stability<sup>[1]</sup>. The simulation curve is shown as follows:

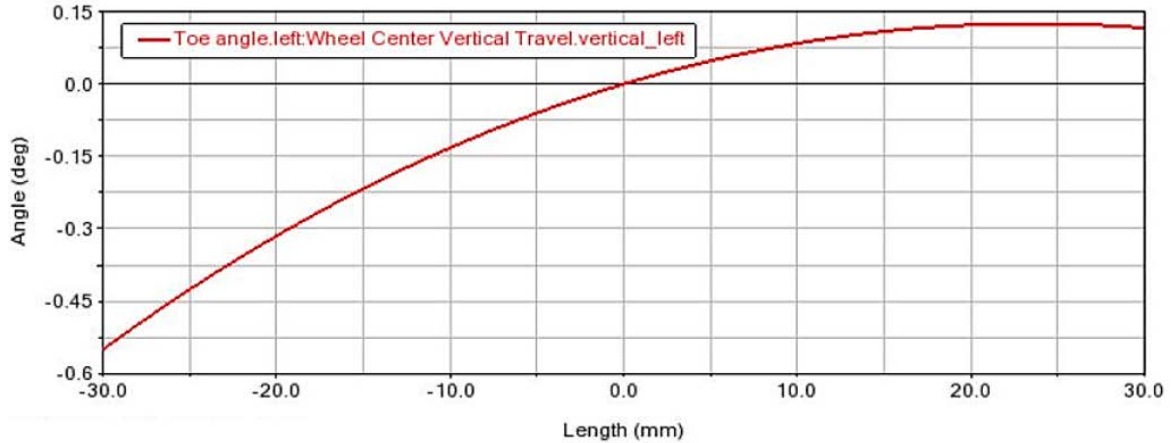


Figure 2: Simulation curve of front-wheel front beam angle.

In Figure 2, it can be seen that the front beam angle roughly shows an upward trend when the wheels jump, with a variation of  $0.65^\circ$ , which is a reasonable range of variation.

### ● Front Wheelbase

The wheel jump occurs when the racing car is driving on undulating road, the wheelbase changes with it, and the tire slides sideways, causing lateral sliding friction, increasing driving resistance, aggravating tire wear, and affecting the vehicle's handling performance, so the wheelbase change should be minimized when designing<sup>[2]</sup>. Therefore, it is usually required that the variation range of unilateral wheelbase should not exceed 10mm, and the wheelbase should be increased when the wheel jumps and decreased vice versa. The simulation curves of the front wheel spacing of the racing car are as follows:

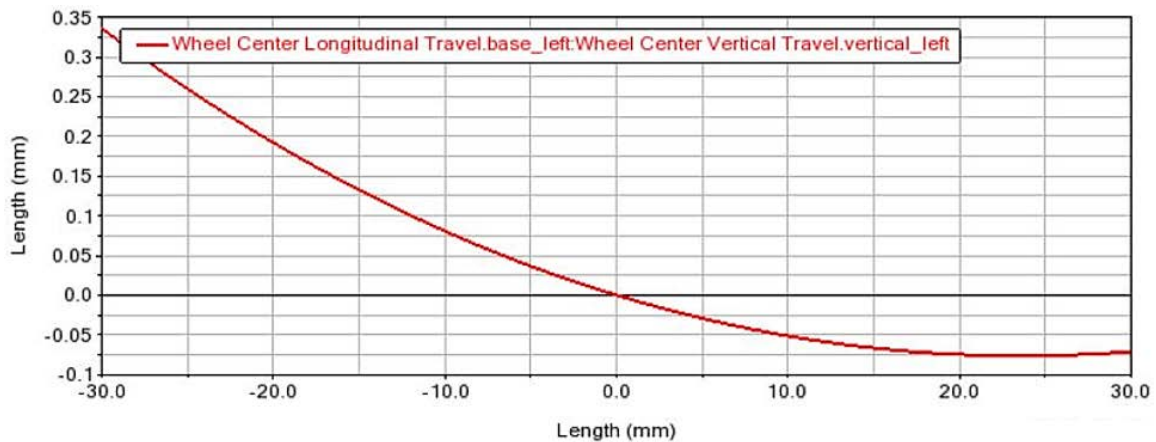


Figure 3: Simulation curve of front-wheel spacing.

From Fig. 3, the wheelbase variation range of the front wheel is 0.405mm, which meets the requirements and the variation trend is also in accordance with the design requirements.

### ● Front suspension roll camber coefficient

The front suspension roll coefficient firstly increases the vehicle's understeering and then decreases it. It can be seen from Fig. 3 that the roll and roll coefficients of the suspension range from 0.888 to 0.935, which are understeering characteristics and meet the design requirements, but the values are too high and need further optimization.

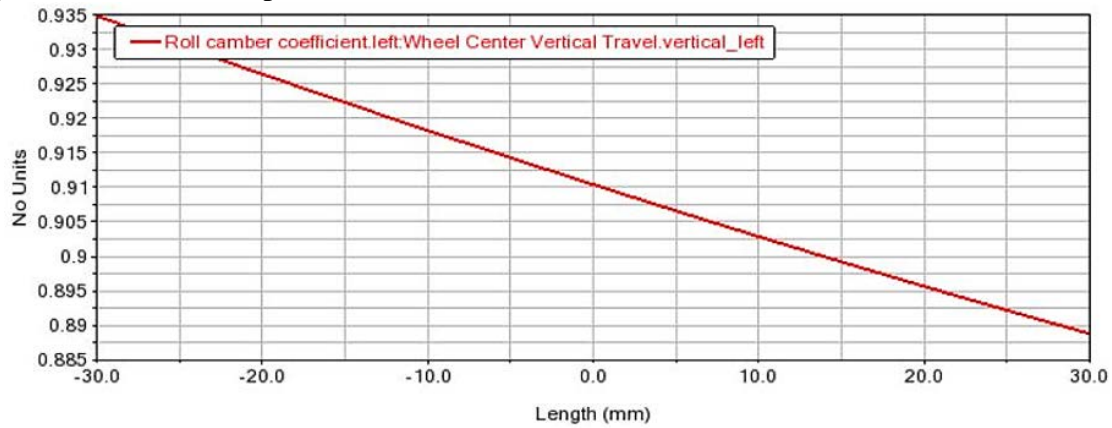


Figure 4: Simulation curve of roll and camber coefficient of front suspension.

### 3.3. Optimization of The Front Suspension

Through the above simulation analysis, it can be seen that the value of the roll camber coefficient is relatively large, so it is taken as the optimization target. Use the Adams/Insight module in Adams's software to perform AB iterations and analyze optimization. Due to the change of the suspension position of the FSAE racing car studied in this paper, the handling stability and ride comfort of the whole vehicle are affected. Therefore, the hard point coordinates of the suspension are selected as optimization variables. The variables that affect the design target parameters include the coordinates of the inner and outer points of the upper and lower cross arms, and the coordinates of the inner and outer points of the tie rod. The column is connected with the hub, caliper, etc., so it cannot be modified, so the outer points of the cross arm and the outer point of the tie rod connected to the column are excluded. To sum up, select the coordinate values of the front and rear inner points of the upper and lower arms of the suspension and the inner point of the tie rod, and analyze a total of 4 parameters. The optimized coordinate values are shown in Table 4:

Table 4: Coordinate values before and after optimization.

| design variable | Before optimization (mm) | Optimized (mm) |
|-----------------|--------------------------|----------------|
| lca_front.z     | 21.85                    | 23             |
| lca_rear.z      | 21.85                    | 23             |
| uca_front.z     | 263.15                   | 265            |
| uca_rear.z      | 263.15                   | 265            |

The optimized suspension model is simulated and analyzed again, and the optimized simulation curve is obtained. Figure 5 is a comparison diagram of the simulation curves of the front suspension roll and camber coefficient before and after optimization. The blue dotted line in the figure is the simulation curve after optimization.



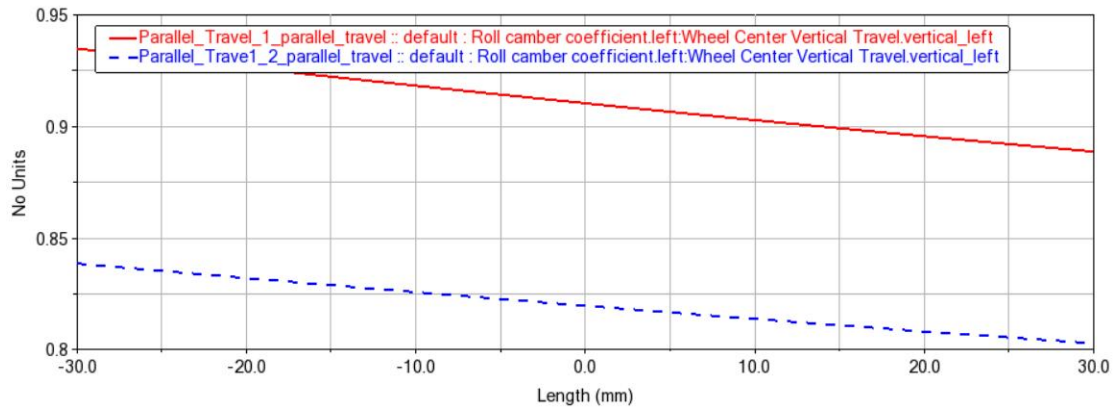


Figure 5: Front suspension roll camber coefficient before and after optimization.

As can be seen from the above figure, the roll camber coefficient after optimization is reduced to between 0.8 and 0.85, and the optimized front suspension structure and performance have been improved to some extent.

#### 4. Finite Element Analysis and Calibration of The Front Suspension of FASE Racing Car

After the ADAMS/Car simulation and ADAMS/insight parameter optimization of the front suspension of the studied FSAE car, the performance parameters of the front suspension are guaranteed to meet the competition requirements. However, it is difficult to accurately calculate the forces and deformation of each part of the column, which is a complex mechanical structure of the FSAE car, when it is driven on the track and other complex road conditions. Therefore, this paper uses ANSYS software to conduct a static finite element analysis of the column of the front suspension of the race car, so as to check whether the design of the column meets the requirements of the competition.

##### 4.1. Introduction and Methods of Finite element method

In the process of automotive design and manufacturing, empirical design and experimental science are closely integrated and complementary. With the wide application of computer-aided engineering (CAE) in the whole cycle of modern automobile development, the cycle time of automobile development has been greatly shortened, the cost has been significantly reduced, and the performance of the whole vehicle has been greatly improved. Among all CAE techniques, the finite element method is considered to be the most widely used and successful engineering analysis technique. Finite Element Method (FEM) is a kind of high-performance calculation method that decomposes the whole object into several finite units for mechanical analysis. The basic idea is to discretize the continuous solution domain into a combination of multiple units connected to each other only at the nodes, with the approximate function assumed in each unit to piecewise represent the unknown field function to be solved on the solution domain, the approximate function is usually represented by the unknown field function and its derivative in the interpolation function of each node of the unit so that a continuous wireless degree of freedom problem into a discrete finite degree of freedom problem. The following figure summarizes the analysis steps of the finite element method:



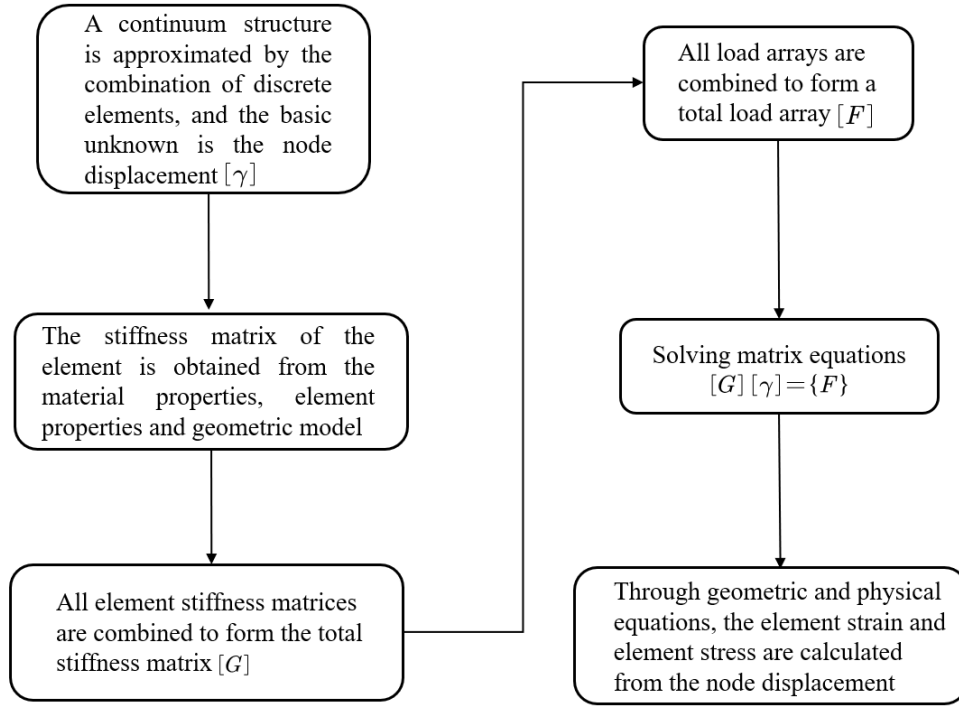


Figure 6: Analysis steps of finite element method.

## 4.2. Static Analysis of The Front Suspension of FSAE Racing Car

Before performing the finite element analysis, it is necessary to use the static analysis method to calculate the forces acting on the main components. According to the description of the column components in "Mechanics of Suspension Components and Chassis" by German scholar Jossen Lemper<sup>[3]</sup>, the force diagram of the interaction between the column and its connecting components is made.

### 4.2.1. Force analysis of the column in the longitudinal plane of the racing car

The force analysis of the column in the longitudinal plane of the front suspension of the racing car is shown in Figure 7 below, where  $F_{PV}$ 、 $F_{PW}$  is the force of the tie rod on the upper cross arm, and point E is the hinge point between the tie rod and the upper cross arm of the front suspension.

From moment equilibrium  $\sum M = 0$  and force equilibrium  $\sum F = 0$  it follows that:

$$F_X + F_{LX} + F_{UX} + F_{PV} = 0 \quad (8)$$

$$F_W e + F_X b + F_{UV}(f - e) + F_{UX} a + F_{PW} g + F_{PV} h = 0 \quad (9)$$

Where:  $F_X$  - the longitudinal force of the ground on the wheel;

$F_{PW}$  - the force of the tie rod on the upper cross-arm in the vertical direction;

$F_{PV}$  - the force of the tie rod on the upper cross arm in the longitudinal direction;

$F_{LX}$  - the force of the lower cross-arm on the column in the longitudinal direction;

$F_{UX}$  - the force of the upper cross-arm on the column in the longitudinal direction;

$f$  - the longitudinal distance between point A and the plane of the wheel;

$e$  - the longitudinal distance between point B and the wheel plane;

$h$  - the longitudinal distance between point E and the wheel plane.  
 After calculation, it is obtained that:  $F_{UV}=196.2\text{N}$ ,  $F_{UX}=-276.8\text{N}$ ,  $F_{LX}=-172.5$ ,  $F_{LV}=586.2\text{N}$ .

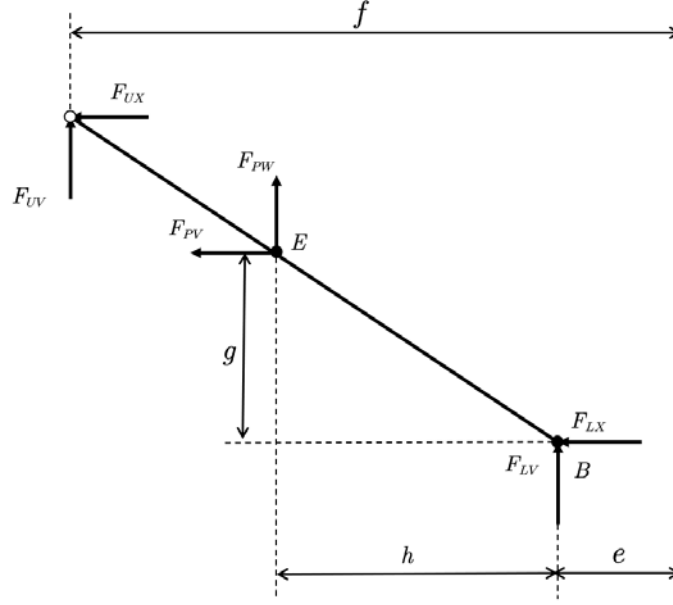


Figure 7: Force diagram of the front column in the longitudinal plane.

#### 4.2.2. Force analysis of the column in the transverse plane of the racing car

The force analysis of the column in the transverse plane of the front suspension of the racing car is shown in Fig. 8 below. points A and B are the articulation points of the upper and lower transverse arms and the column, respectively. To facilitate the calculation, we establish a two-bit coordinate system and decompose the forces at each point along the coordinate axes of the Cartesian coordinate system.

From the equilibrium of forces in a single direction  $\Sigma F = 0$  can be obtained:

$$\begin{cases} F_W + F_{UV} + F_{LV} = 0 \\ F_H + F_{LH} + F_{UH} = 0 \end{cases} \quad (10)$$

From the balance of moments at points A and B, we get:

$$\begin{cases} F_W d + F_H (a + b) + F_{LV} (d - c) + F_{LH} a = 0 \\ F_W c + F_H b + F_{UV} (d - c) + F_{UH} a = 0 \end{cases} \quad (11)$$

Where:  $F_W$  -the vertical force of the ground on the tire;

$F_H$  -the lateral force of the ground on the tire;

$F_{UV}$  -the vertical force of the upper cross-arm on the column;

$F_{UH}$  -the lateral force of the upper cross-arm on the column;

$F_{LV}$  -the vertical force of the lower cross-arm on the column;

$F_{LH}$  -the lateral force of the lower cross-arm on the column;

- a-the distance between points A, B in the vertical direction;
- b-the vertical distance between point B and the ground in the vertical direction;
- c-the distance between point B and the longitudinal center of the wheel;
- d-the distance between point A and the longitudinal center of the wheel.

After calculation, it is obtained that:  $F_W=627.3\text{N}$ ,  $F_{UV}=-653.6\text{N}$ ,  $F_{LV}=26.3\text{N}$ ,  $F_{UH}=256.3\text{N}$ ,  $F_{LH}=-256.3\text{N}$ ,  $F_H=-243.6\text{N}$ .

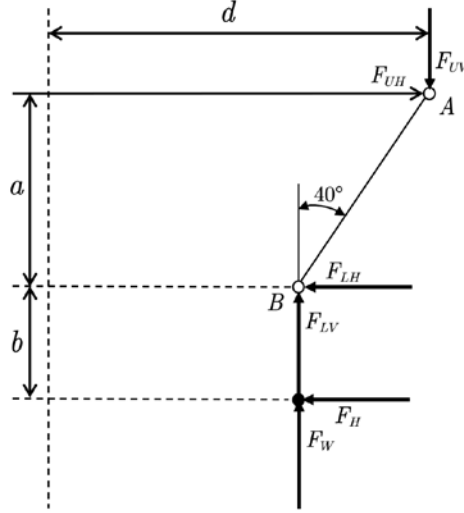


Figure 8: Force diagram of the front column in the transverse plane.

### 4.3. Finite Element Analysis of The Suspension Column

#### 4.3.1. Modeling

The geometric model is the first step of FEA. There are two ways to build the geometric model for FEA: (1) to build the geometric model by SolidWorks, Catia, UG and other 3D modeling software, and then import it into FEA software; (2) to build the geometric model directly in ANSYS. These two methods have their advantages and disadvantages: the first method has the advantage of easier and shorter modeling, but the mesh division after importing the model into ANSYS is prone to line and surface fractures, resulting in mesh quality degradation. The second way is more complicated to build the model directly in ANSYS than with professional 3D software, but the quality of the created mesh is higher and the subsequent calculation results are more accurate. Therefore, simple models are usually built directly in ANSYS, while models with more complex structures are generally modeled in 3D software and then imported for analysis.

In the actual modeling process, we often come across models with complex structures, and it is obviously unnecessary or impossible to build them exactly according to the actual model structure. Therefore, in this paper, when building the column model, the geometric model is appropriately simplified based on the results of the finite element analysis. The simplification of the geometric model is usually done according to the following principles.

- (1) Appropriate simplification is performed for models with complex profiles.
- (2) Appropriate simplification can be performed for the non-load bearing part of the model, which will not affect the results of FEA, and at the same time will make the FEA faster and improve the efficiency of FEA.
- (3) Appropriate simplification of the non-major structural features of the model. Such as modeling ignore the small size of the flange, small holes or reinforcement ribs. The reason for this treatment is because when meshing in ANSYS, these smaller size secondary structures will appear as cells with

too small an angle, and make the cell quality severely degraded and undesirable phenomena such as stress concentration and stress singularity.

In this paper, the modeling process was appropriately simplified by following the above principle, and the left and right column models are shown in the figure below were created using Catia. The column models were saved in Catia as "stp" format, and then the models were imported directly through the ANSYS interface.



Figure 9: Front suspension left column model.

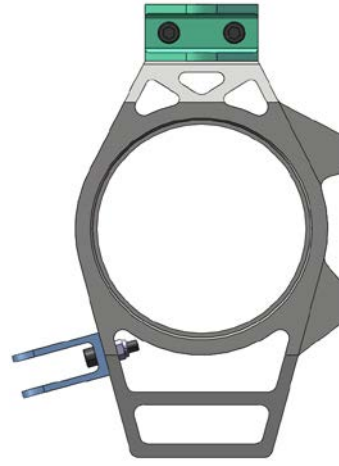


Figure 10: Front suspension right column model.

#### 4.3.2. Material Properties and Unit System

In this paper, 4310 structural steel was selected as the raw material for the column analysis, and the material property parameters set in ANSYS for the front suspension column are given in the following table.

Table 5: Material properties of 4310 structural steel.

| Material Properties         | Parameters            |
|-----------------------------|-----------------------|
| Density $\rho$              | 7850kg/m <sup>3</sup> |
| Modulus of elasticity $E$   | 205GPa                |
| Poisson's ratio $\mu$       | 0.285                 |
| Tensile strength $\sigma_b$ | 950Mpa                |
| Yield strength $\sigma_s$   | 810Mpa                |

When performing finite element analysis through ANSYS, it is usually necessary to enter only the values of physical quantities without setting the units. In this paper, for the accuracy of the analysis results, a set of units must be set in ANSYS to ensure the uniformity of the units. Since the length unit of the model in Catia is mm, the units used in this paper are: (i) length unit is set to millimeter (mm), (ii) mass unit is set to kilogram (kg), (iii) force unit is set to newton (N), and (iv) stress unit is set to megapascal (MPa). Such unit setting can avoid the error of results caused by the inconsistency of units in the subsequent analysis.

### 4.3.3. Cell selection and Meshing

Before meshing, the model needs to be selected for the cell type. The three-dimensional solid model of the column established in this paper should use three-dimensional solid cells. three-dimensional solid cells in ANSYS are divided into many cell types according to the nodes and degrees of freedom, usually divided into tetrahedral cells and hexahedral cells. Among them, the hexahedral unit in the analysis has better results than the tetrahedral unit, while the number of discrete units of the hexahedral unit is also much less than the number of discrete units divided into tetrahedral units, such a discrete division is more conducive to computer operations. However, the use of hexahedral unit division of the three-dimensional entity requirements are higher, the required division of the three-dimensional model should be more regular, relatively few transition surfaces, solid surface to be relatively regular. Therefore, for the surface structure of complex solid models usually use tetrahedral cells for meshing. In this paper, SOLID92 is taken as the type of unit. SOLID92 is a tetrahedral ten-node structural unit, each node contains three degrees of freedom (respectively, translation along x, y, z), as shown in Figure 11. Because the SOLID92 unit has a quadratic displacement function, it is more suitable for meshing irregular models, especially those with professional 3D software drawing. The unit has both stress rigidity, shaping, large deflection, expansion and large tension, which are suitable for the unit type of the model in this paper.

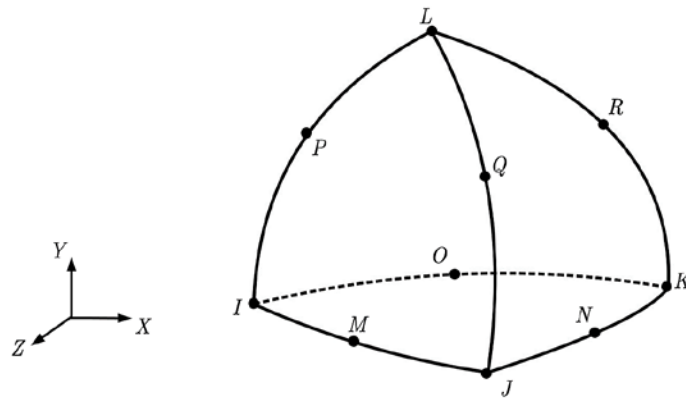


Figure 11: Cell type of SOLID92.

The meshing in ANSYS can be divided into the following two types: free meshing and mapped meshing, as shown in Figure 12. It is important to adopt that type for meshing. When free meshing is used, there are no specific restrictions on the shape of the divided entities, and there are no strict requirements and restrictions on the shape of the cells. In contrast, the division of mapping mesh requires strict requirements on the model and cell shapes, and a mapping surface can be divided into either triangular cells only or quadrilateral units only. However, the model to be mapped can only be divided into regular tetrahedral or hexahedral units. Therefore the model to be partitioned using the mapping mesh must be composed of regular faces or bodies.

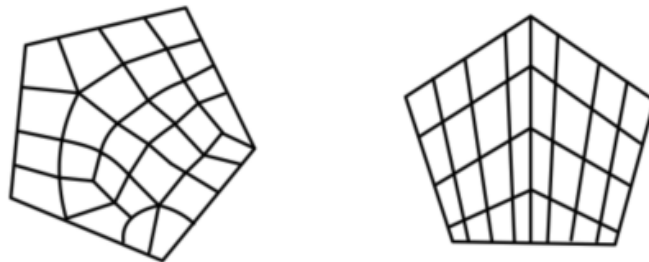


Figure 12: Free and mapped meshes.

For the complex column model established in this paper, tetrahedral free meshing should be used, and local refinement should be carried out to make the overall mesh more uniform after the automatic mesh division is completed for the parts with low division quality. The finite element model after meshing is shown in Figure 8 and Figure 9. The left column model of the front suspension has 509472 nodes and 311674 cells; the right column model of the front suspension has 508786 nodes and 311171 cells.

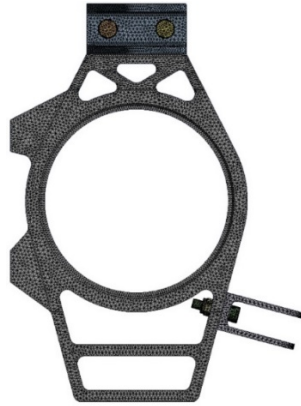


Figure 13: Grid of the left column of the Front Suspension.



Figure 14: Grid of the right column of the Front Suspension.

#### 4.3.4. Load Application on The Front Suspension Column

In the wheel side assembly of the front suspension, the column is interconnected with the suspension, steering system, transmission system and braking system of the racing chassis. Take the left column of the front suspension as an example, the left side of the column is connected to the cross-tie ball head assembly for steering control, and the right side of the column is fixed to the caliper of the brake system, and its upper and lower ends are connected to the upper and lower cross arms respectively. When constraining the boundary conditions of the column, it is necessary to clarify the interconnection between the column and the connected parts<sup>[4]</sup>.

The type of suspension selection determines the type of column. The type of suspension designed in this paper is double-wishbone independent suspension. The steering tie rod of the steering system brings the motion and force of the steering action to the column to make the front wheels turn, which is equivalent to the column being the end of the transmission part of the racing steering system and belongs to the actuator of the racing steering system.

And, as can be seen from the assembly diagram of the front suspension wheel side system of the racing car, the column and the caliper are fastened together by hexagonal bolts, and also connected to the wheel hub through the chuck, thus forming a one-piece mechanism. When the car brakes, the caliper tightens the chuck, and there is restraint and load transfer between the column and the caliper.

By appealing to analyze the connection between each part and the column, we can deduce the following: ① the column steering lug is connected to the steering tie rod through the pin, and they are hinged; ② the two one-piece lugs on the side of the column and the caliper are connected through the bolt; ③ the lugs on the upper and lower ends of the column are connected to the joint bearings at the ends of the upper and lower cross arms through the ball pins; ④ the center hole of the column fits the wheel hub assembly, and the wheel hub is connected to the vehicle as well as the inner ring of the large hole of the column, and they are bearing connections.

The load in ANSYS contains the boundary conditions as well as the external (intrinsic) forces. The magnitudes of the loads have been calculated in the previous section and the loads are applied to the



corresponding points or surfaces in the form of average pressures. In the following, we analyze the column for two typical conditions of a racing car under braking and cornering. The situation after applying the applied forces and constraints at each point is shown in Fig. 15 and Fig. 16.

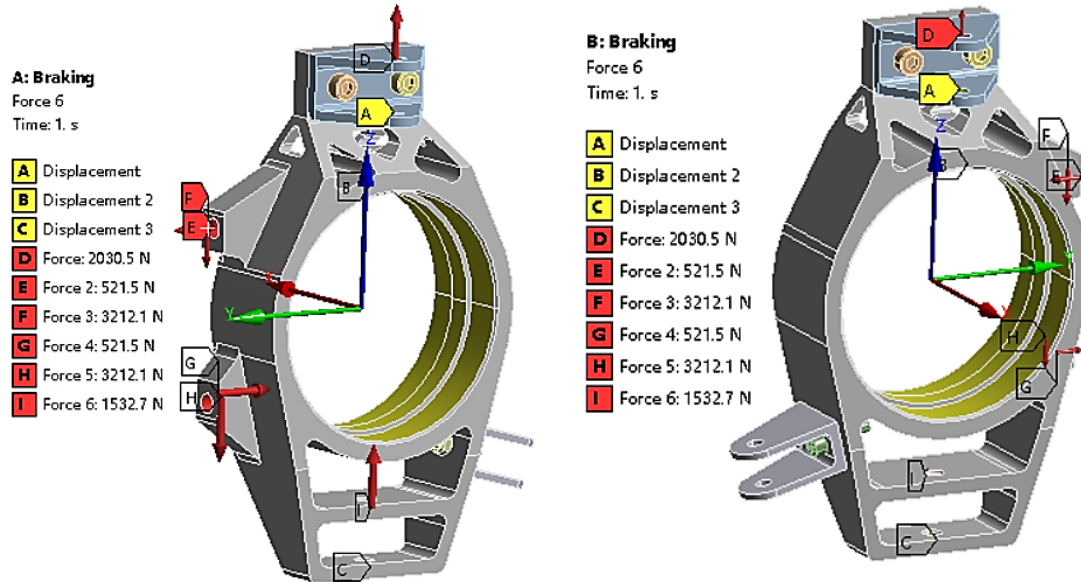


Figure 15: Force on the left and right columns of the front suspension during braking.

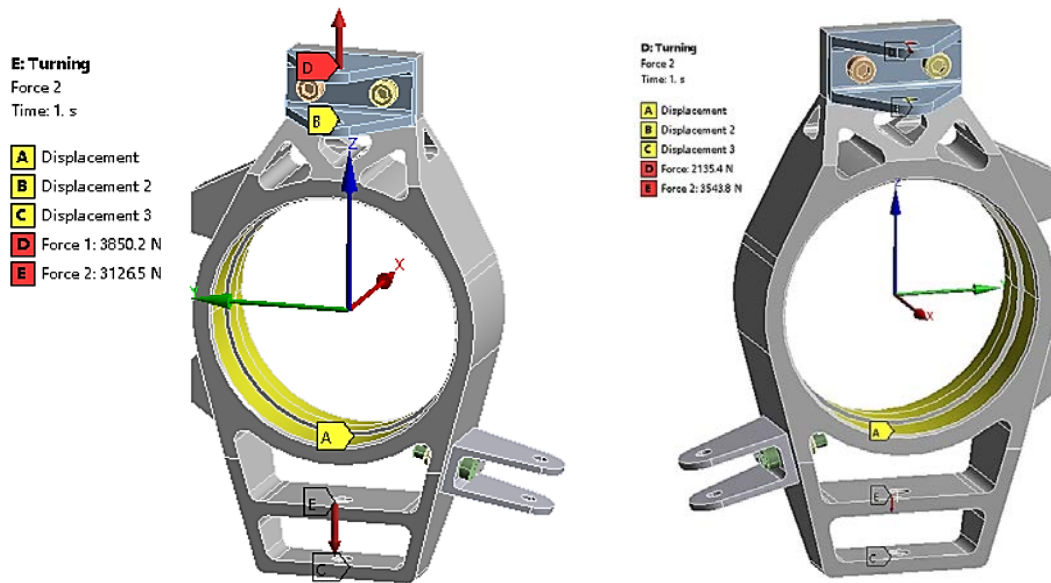


Figure 16 Front suspension left and right column forces during cornering.

#### 4.3.5. Finite Element Analysis of The Front Suspension Column

After applying the above constraints and loads to the column, the solution is started. After the solution is completed, it enters the post-processing module and the final analysis graph is obtained. The knot analysis in this paper mainly contains the total displacement-deformation diagram and the stress diagram of the model.

### (1) Analysis of braking conditions

The deformation and stress diagrams of the left and right columns of the front suspension under braking conditions are shown in Figures 17 and 18. The maximum deformation of the left column occurs at the edge of the outer end of the lifting lug connected to the upper cross arm, and the maximum deformation is 0.833mm, which can meet the stiffness requirement of the column. The maximum stress of the left column is generated in the area where the upper end of the upper lug is connected to the column. The maximum equivalent force is 437.64 MPa, which is less than the yield limit of the material 810 MPa. The stress surface becomes larger at the connection of the lower cross arm under the influence of load transfer.

The maximum deformation of the right column of the racing car also occurred at the edge of the outer end of the lugs connected to the upper cross arm, and the maximum deformation was 0.294mm, which could meet the stiffness requirement. The maximum equivalent force of the right column is 436.27Mpa, which is less than the yield limit of the material, indicating that the designed front suspension left and right columns structure and material can meet the requirements in braking conditions.

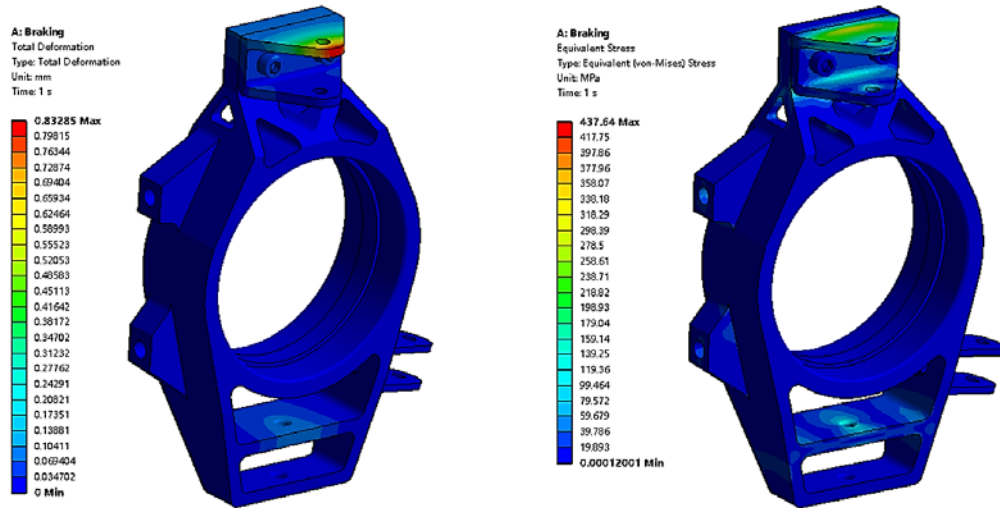


Figure 17: Strain and stress clouds of the left column of the front suspension during braking.

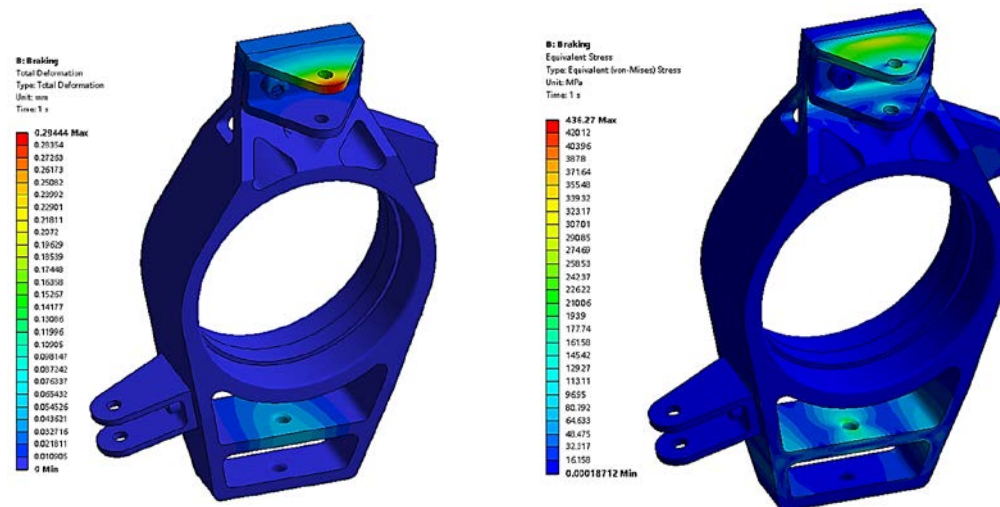


Figure 18: Strain and stress clouds of the right column of the front suspension during braking.

## (2) Analysis of steering conditions

The deformation and stress diagrams of the left and right columns of the front suspension during steering are shown in Figures 19 and 20. The maximum deformation of the left column also occurs at the edge of the outer end of the lifting lug connected to the upper cross arm, and the maximum deformation is 1.629mm, which can meet the stiffness requirement of this structure. The maximum equivalent of the left column also occurs at the upper end of the upper lug and the column connection area. The maximum equivalent stress is 664.07 MPa, which is less than the yield limit of 810 MPa, and the stress surface becomes larger at the lower cross-arm connection due to load transfer.

The maximum deformation of the right column of the racing car occurs in the connection area with the lower cross arm, and the maximum deformation is 0.219mm, which can meet the stiffness requirement. The maximum stress of the right column in the steering condition also occurs in the area connected with the lower cross arm, and the maximum equivalent force is 333.01Mpa, which is less than the yield limit of the material. It means that the structure and material of the left and right columns of the front suspension can meet the requirements of the steering condition.

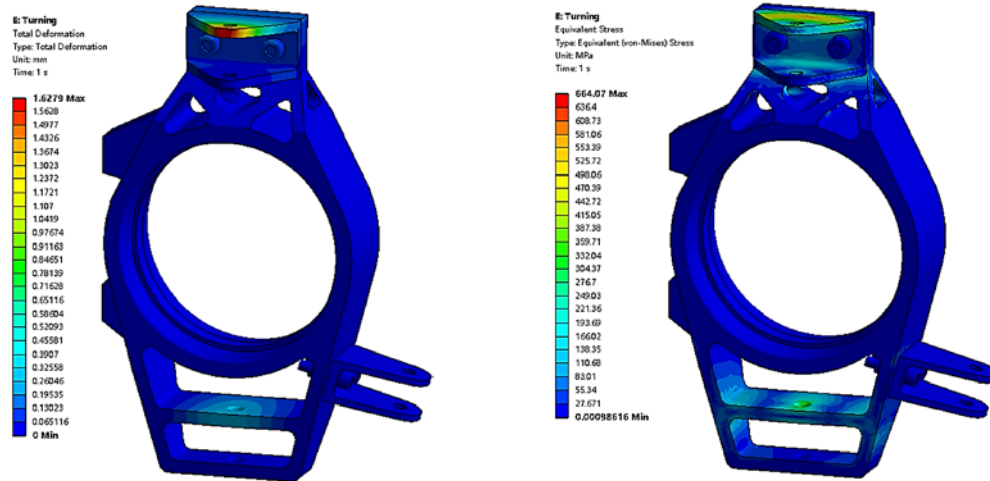


Figure 19: Strain and stress clouds of the left column of the front suspension during steering.

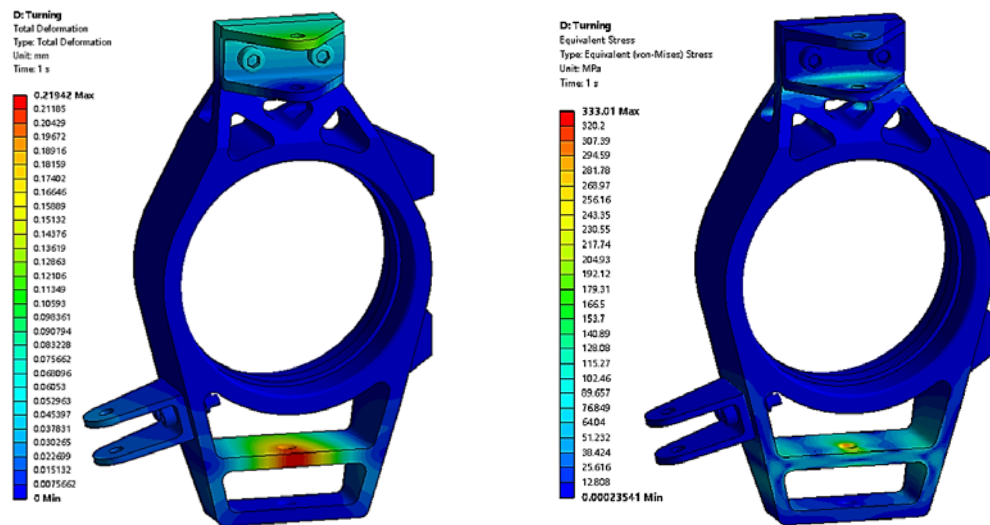


Figure 20: Strain and stress clouds of the right column of the front suspension during steering.

In summary, the column model designed in this paper can meet the deformation and strength requirements of the material. However, through the strain and stress diagram of the column, it can be found that the stress is concentrated at the outer edge of the lugs connected to the upper cross-arm of the column, and this situation will cause stress fatigue and damage to the lugs if it lasts for a long time. Such as in the stress concentration parts welding reinforcement can effectively improve the distribution of stress, to prevent stress concentration and other phenomena. At the same time, the wall thickness can be appropriately reduced in the area where the stress concentration is small, such as the stress around the bearing hole where the column is connected to the hub, which can effectively reduce the weight of the column, saving costs and reducing the load of the car.

## 5. Conclusion

In this paper, the design and Catia modeling of the front suspension of the race car were carried out with the background of the Formula Student Automobile Competition FSAE in China. The virtual simulation model of the suspension of the racing car was established in ADAMS/Car environment using the multi-body system dynamics theory method, and the dynamics simulation analysis of the suspension was carried out, and ADAMS/Insight was used to optimize the relevant parameters. Then, the finite element models of the left and right columns of the front suspension were created by ANSYS software using the theory and method of finite element, and the stress and deformation analysis were carried out to ensure that the column models could meet the deformation requirements and strength requirements of the material.

## References

- [1] Qian Silei, Mei Xueqing, Su Wenhong. Kinematic simulation and parameter optimization of the front suspension of FSAE racing car[J]. *Automotive Practical Technology*, 2021, 46(05): 125-128. DOI: 10.16638/j.cnki.1671-7988.2021.05.036.
- [2] Han Zhaohui. Simulation analysis of automotive suspension system based on ADAMS and MATLAB [J]. *Mechanical Design*. 2008, 7: 11-14.
- [3] Jelsen Reimpauer, translated by Wang Xuan. *Suspension components and chassis mechanics [M]*. Changchun: Jilin Science and Technology Press, 1992.
- [4] Liu M, Zhu RF, Qiao XL. ANSYS-based simulation analysis of FSAE racing car[J]. *Applied Science and Technology*, 2021, 48(02): 87-94.